

See discussions, stats, and author profiles for this publication at: <https://www.researchgate.net/publication/276130325>

Spatial Heterogeneity of Glassy Polymer Films

ARTICLE *in* MACROMOLECULES · APRIL 2015

Impact Factor: 5.8 · DOI: 10.1021/ma502610u

CITATION

1

READS

13

4 AUTHORS, INCLUDING:



Igor Siretanu

University of Twente

16 PUBLICATIONS 69 CITATIONS

SEE PROFILE

Spatial Heterogeneity of Glassy Polymer Films

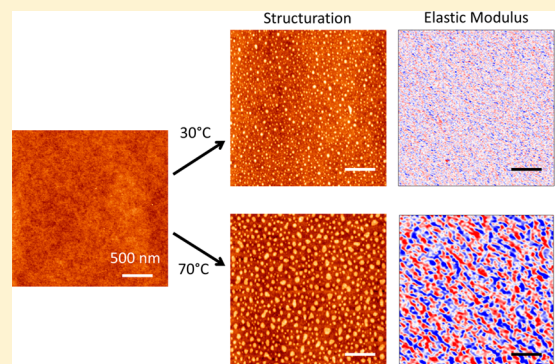
Igor Siretanu,[†] Hassan Saadaoui,^{‡,§} Jean-Paul Chapel,^{‡,§} and Carlos Drummond*,^{‡,§}

[†]Physics of Complex Fluids, MESA Institute for Nanotechnology, University of Twente, Post Office Box 217, 7500 AE Enschede, The Netherlands

[‡]Centre de Recherche Paul Pascal (CRPP), CNRS, UPR 8641, F-33600 Pessac, France

[§]Centre de Recherche Paul Pascal, Université de Bordeaux, F- 33600 Pessac, France

ABSTRACT: By studying the morphology of polystyrene films subjected to a fast structuration method, we demonstrate the spatial heterogeneity of their surface viscoelasticity at temperatures well below the glass transition temperature, T_g . Our results point to a nonrandom arrangement of zones of different elastic modulus deep in the glassy state. The spatial distribution of viscoelastic properties of the film was temperature dependent; we observed the presence of soft zones (surrounded by areas of larger elastic modulus) spanning increasingly larger areas of the surface as T gets closer to T_g . The heterogeneity on viscoelastic properties of the film is supported by the temporal evolution and relaxation of the structured surfaces and by direct measurements of the spatial distribution of the local elastic modulus of polystyrene films.



INTRODUCTION

The physical description of the glass transition is a longstanding problem that continues to attract the attention of many research groups. Probably the most significant indication of this transition is the enormous increase of viscosity as the temperature T approaches the glass transition temperature T_g in glass-forming liquids. This fact has been extensively discussed in the literature; the absence of significant structural evolution accompanying the dramatic slowing down of the relaxation times close to T_g continues to be particularly puzzling.^{1–3}

Two aspects of the glass transition have attracted great interest in the past few decades. One is related to the relaxation dynamics (often characterized by a temperature-dependent relaxation time, τ) of glass-forming systems above and below T_g . It is generally accepted that as T approaches T_g from above, the increasing relaxation time can be well described by empirical expressions like the Vogel–Fulcher–Tamann (VFT) or its equivalent Williams–Landel–Ferry, which predict a divergent τ at a particular temperature below T_g .^{1,3} Nevertheless, the accuracy of these “laws” at the glassy state ($T < T_g$) has been questioned; significant deviations of the behavior of τ with respect to the VFT model have been observed in experimental studies; in parallel, theoretical works have proposed a weaker increase of τ below T_g .^{3,4} A second aspect which has been extensively discussed in the recent literature is the validity of describing the dynamic of the glass transition by a simple relaxation process. Indeed, a more complex scenario appears to be the rule rather than the exception when T is close enough to T_g . A number of reports signaling that the dynamics of supercooled liquids become heterogeneous close to the glass transition can be found in the

literature.^{5–8} Some excellent reviews about this subject have been published.^{4,7,9}

It is reasonable to expect that the dynamic heterogeneity of the liquid will be reflected in the properties of the glass; however, this aspect has been less investigated. As the relaxation times on the glass state are naturally very long, these studies are very time-consuming. In addition, the properties of nonequilibrium glasses depend on the previous history of the material and on details of the experimental protocol, making it difficult to precisely control and report the results. Some studies that hint dynamic spatially heterogeneity in polymer glasses has been recently reported. Thurau and Ediger studied the aging of polystyrene PS films at temperatures far below T_g and concluded that the dynamic of the glassy film was spatially heterogeneous.¹⁰ Riggelman and co-workers reached a similar conclusion in a study of deformed polymer films.¹¹ Vallée and co-workers reported spatial heterogeneity of the dynamic of two polymers at temperatures below T_g from measurements of the lifetime of the fluorescence of molecular probes added to the polymers.¹²

In this work we investigated the dynamics of glassy PS films by studying the relaxation of small surface deformations. We have recently shown that when glassy PS films are put in contact for a few minutes with a degassed water solution containing adsorbing ions, a long-lasting nanostructuration spontaneously forms on the solid surface.^{13,14} This process, which is controlled by the dissolved ions, occurs only after the concentration of dissolved gases in the aqueous phase is

Received: December 29, 2014

Revised: March 2, 2015

Published: April 10, 2015

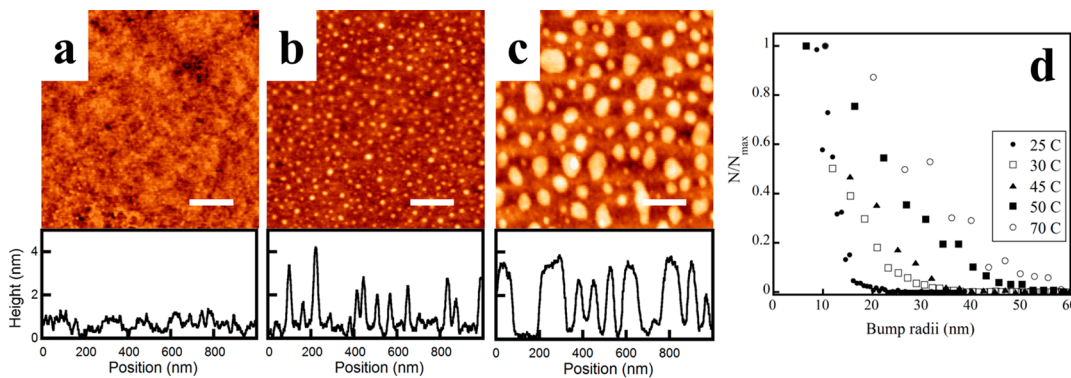


Figure 1. $1 \mu\text{m} \times 1 \mu\text{m}$ height tapping mode AFM micrographs taken in air of 300 nm thick 250 kDa PS films after exposure to (a) nondegassed and (b, c) degassed solutions of nitric acid in double distilled water at pH 1.5. The temperature during treatment was (a, b) 25 °C and (c) 70 °C. A typical height profile for each condition is presented. The presence of self-assembled asperities (bumps) is observed only on the surfaces exposed to the degassed solution for 1 min. The scale bars correspond to 200 nm. (d) Normalized bump size distribution for different temperatures during surface treatment with degassed acid water.

reduced, favoring the contact between the charged ions and the hydrophobic surface. We have shown in the past that this process involves the rearrangement of polymer molecules to depths of the order of the polymer size.¹⁵ The surface structuration occurs in less than a minute; thus, this method, which we called ion-induced polymer nanostructuration, IPN, allows us to obtain a snapshot of the spatially resolved surface elasticity of the polymer film, as described below.

MATERIALS AND METHODS

Atactic polystyrene (PS) of 250 kg/mol (T_g 103 °C, measured by DSC) was obtained from ACROS Organics and used as received.

Film Preparation and Treatment. We prepared films of 300 nm of PS on thoroughly cleaned silicon wafers by spin-coating from toluene solutions. Wafers were covered with a monolayer of 10 nm diameter ceria nanoparticles before polymer coating to increase the adhesion between the polymer layer and the substrate.¹⁶ Some films were prepared without the ceria layers to corroborate that the results reported are independent of the presence of this primer layer. The films were annealed at 95 °C for 10 h—to completely remove the solvent and to favor the relaxation of residual stress—and cooled down to room temperature. The thickness of the films was determined by ellipsometry (Nanofilm). Root-mean-square roughness smaller than 0.5 nm (measured by AFM in $1 \mu\text{m}^2$ images) was typically observed after annealing. The films were subsequently equilibrated at a given temperature and then exposed for 1 min to degassed double distilled water at pH 1.5 (with HNO₃) pre-equilibrated at the same temperature. Then the films were dried with a gentle flow of N₂ gas and cooled back to room temperature. In some rare cases water penetrated between the polymer film and the substrate. These samples were not further considered. After structuration and drying, the films were aged following different protocols, as explained below.

Water Degassing. Millipore water with resistivity of 18 MΩ cm was used for preparing the acid solutions. The pH of the aqueous phase was adjusted to 1.5 by adding small amounts of nitric acid (Aldrich) as necessary. Carefully cleaned Teflon bar stirrers were introduced in the solutions to be degassed to induce the nucleation of gas bubbles. The solutions were subjected to agitation under pressure of 0.2 mbar for 2 h. The appearance of macroscopic bubbles in the aqueous phase was observed only during the first 30 min of degassing. After degassing was finished, the air pressure on the flask was gently increased back to atmospheric pressure.

Film Characterization: Morphology and Elastic Modulus. The polymer morphology after nanostructuration and aging was examined by tapping mode AFM (Icon, Bruker) and characterized by the average size and height of the self-assembled polymer bumps present on the surface. To characterize the local elastic properties of

nontreated films, experiments were carried out in a Cypher ES Environmental AFM with blueDrive photothermal excitation¹⁷ (Asylum Research/Oxford Instruments, Santa Barbara, CA) in AM-FM (amplitude modulation–frequency modulation) viscoelastic mapping mode using AC160TS probes (Olympus). In this mode, two cantilever resonances are simultaneously measured and three feedback loops are implemented. First, by using the main cantilever resonance (operating in AM) topographic information is obtained. A second lock-in measures the phase and amplitude at a higher cantilever resonance, operating in FM mode at much smaller oscillation amplitude. An automatic gain control circuit monitors the amplitude and adjusts the drive voltage to keep the amplitude constant. A phase-locked loop monitors the phase and adjusts the drive frequency to keep the phase at 90° to measure the shift in resonance frequency. The output resonance frequency is related to the elastic tip–sample interaction; basically, higher resonance frequency means greater contact stiffness. The final feedback maintains constant the amplitude of oscillation of the second mode; this information is used to calculate the tip–sample stiffness.^{18,19} Hence, a quantitative elasticity map (elastic modulus) can be obtained from frequency, amplitude, and phase of two modes by using a contact mechanics model. Samples were placed in an environmental scanner equipped with a heating stage and were investigated so that probe tapping was in repulsive mode at a phase less than 50° for the AM pass. Samples were imaged at a scan rate of 4 Hz. To calibrate the response of the system, we measured the elastic modulus of a polystyrene sample provided by Bruker (PSFILM-12M, 2.7 GPa).

RESULTS AND DISCUSSION

Atomic force microscopy micrographs illustrating the IPN phenomenon are presented in Figure 1. The observed patterning is a consequence of surface instability due to the adsorption of ions (e.g., hydronium) at the polymer–water interface. The resulting deformation and its ulterior relaxation are determined by the viscoelastic properties of the film. As can be observed in Figure 1, the typical size of the self-assembled pattern depends strongly on the temperature during treatment. We can distinguish two different scenarios. At low temperature ($T < 30$ °C) a monomodal bump size distribution is observed. On the contrary, the size distribution increasingly broadens as the temperature of treatment is increased. The broad distribution is observed right after the treatment; it does not seem to be a consequence of the temporal evolution of the polymer surface. We can identify zones of smaller and larger bump sizes which are not regularly distributed on the surface, although no structural heterogeneity could be observed in the

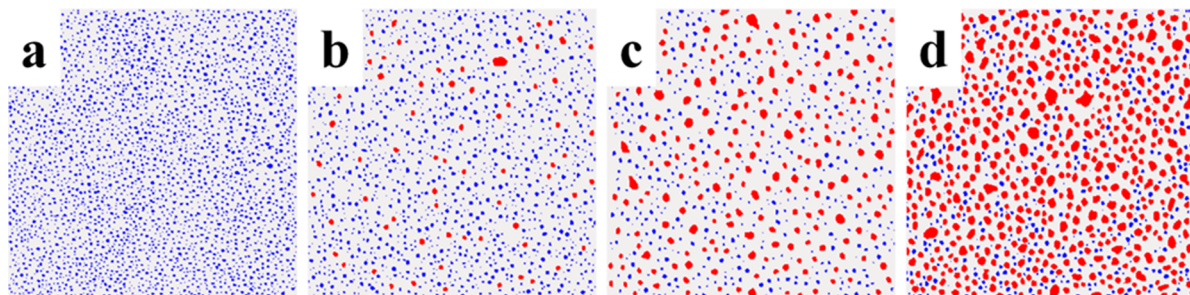


Figure 2. $3\text{ }\mu\text{m} \times 3\text{ }\mu\text{m}$ height tapping mode AFM micrographs taken in air of 300 nm thick 250 kDa PS films after exposure to degassed solutions of nitric acid in double distilled water at pH 1.5. The temperature during treatment was (a) 25, (b) 30, (c) 50, and (d) $70\text{ }^{\circ}\text{C}$. Bumps with radii larger than 30 nm are colored red; otherwise, they are colored blue.

morphology of the films before the treatment. It seems impossible to determine by simple inspection of the unstructured films where regions of small or large bump size will appear. As can be observed in Figure 1, the areal fraction occupied by large bumps increases with temperature of treatment, occupying most of the surface at $70\text{ }^{\circ}\text{C}$; however, zones of small bumps ($r < 30\text{ nm}$) can always be identified. As mentioned, the bump distribution is not completely random. This is more clearly visible in larger size AFM micrographs, as the ones presented in Figure 2. The generated bumps were split by size in two populations, larger and smaller than 30 nm . It is clear that at high T the small bumps form a network on the polymer surface (the observed patterns do not depend significantly on the size chosen for splitting the bumps). This network traverses the whole surface area at all temperatures investigated, even when the zones with large size bumps vastly overweight the regions showing small size deformation.

There is a large body of literature devoted to the description of the deformation of films under the influence of an external disrupting force.^{20,21} Other than the applied stress, the deformation of the polymer film will be determined by the elastic shear modulus of the film, μ , and the stabilizing Laplace pressure, controlled by the water–PS interfacial tension, γ_{int} . The characteristic size of the resulting deformation is rather independent of the viscosity, η , which determines the rate of formation and eventual relaxation of the patterned film.^{20,21} It seems reasonable to assume a homogeneous value of γ_{int} for the films (this is rather inconsequential, as the effect of the capillary force is very small with respect to the elastic force). Thus, the fast structuration process can be used to evaluate the spatial variability of μ at the moment of the treatment. The observed heterogeneous deformation at high temperatures is an indication of μ heterogeneity: larger (smaller) characteristic deformation lengths can be related to smaller (larger) local μ values. Interestingly, assuming that continuum mechanics models discussed in the literature can be applied to the system under study, the observed increase in the typical self-assembled bump size (a factor between 3 and 4; cf. Figure 1) translates into a large reduction of several orders of magnitude in μ .^{20,21}

Dynamic nonuniformity in thin glassy polymer films has often been discussed in terms of dependence of chain mobility on the distance from the film boundaries. The idea of enhanced polymer mobility close to the surface or a surface-induced polymer mobility gradient^{22,23} has been extensively discussed in the literature, after the seminal work of Keddie and co-workers evidencing a film thickness dependence of T_g .²⁴ However, the films are commonly considered homogeneous in the plane. On the contrary, as mentioned above, it is getting increasingly clear

that as a glass-forming liquid approach T_g , a correlation length scale emerges and it becomes dynamically heterogeneous: the relaxation times in a liquid near T_g can vary by several orders of magnitude between neighboring regions.^{7,9} This idea can be traced back conceptually at least to the model of cooperative rearranging regions advanced by Adams and Gibbs²⁵ and experimentally confirmed through 4D-NMR experiments with poly(vinyl acetate) above T_g .²⁶ It is then reasonable to expect that spatial heterogeneities may also be present in the glass, influencing material properties and aging process. It seems erroneous to attribute the heterogeneity observed in this work just to the quenching of a nonhomogeneous liquid: all the films were stored at room temperature before treatment at a particular temperature; thus, they were viscoelastically homogeneous (within the spatial resolution of our experimental methods) before being treated at high temperatures, as can be inferred from Figure 2a. It seems that softer zones appear at temperatures above $30\text{ }^{\circ}\text{C}$, progressively growing all around the film as T gets closer to T_g ; the films become increasingly spatially heterogeneous when T increases. This progression is confirmed by direct elastic modulus measurements described below.

The heterogeneous structuration of the PS films at $T > 30\text{ }^{\circ}\text{C}$ indicates that the viscoelastic properties of the film change from place to place on the surface. In this direction, it has been recently reported that more than one equilibration mechanism with very different time scales are present in aging glassy PS films.²⁷ In the same line, theoretical description of aging glasses (simulated by reducing temperature from $T > T_g$ to $T < T_g$) in the framework of the random first-order transition (RFOT) theory predict a heterogeneous dynamics, with a bimodal distribution of relaxation times. Dynamical heterogeneity is also naturally predicted by kinetically constrained models: the clustering of slow and fast zones appears as a consequence of fast (slow) regions, promoting (obstructing) the movement and relaxation of their neighbors.²⁸

We also investigated the temporal evolution of the self-assembled bumps. In a first test, a number of samples were structured under identical conditions at $25\text{ }^{\circ}\text{C}$, so an initial monodisperse bump size distribution was obtained. To exclude potential substrate effects on the near surface dynamics, the PS films were relatively thick ($h = 300 \pm 20\text{ nm}$). Two methods were used to explore the dynamics of the structure relaxation. At low annealing temperatures we measured the size distribution of a number of samples with identical preparation, thermal history, and the same treatment with degassed solution, analyzing each sample only once. This procedure was repeated at different annealing times until bumps were no longer

observed and the polymer films recovered their original smoothness. The second procedure, used for studying the nanostructure relaxation at high temperatures ($T > 70$ °C), consisted in following the morphology of the polymer surfaces in real time, by placing the samples on the AFM heating stage and measuring the bump relaxation *in situ* by repeated scans.

The temporal evolution for mean bump height at different temperatures below T_g is presented in Figure 3a; as can be

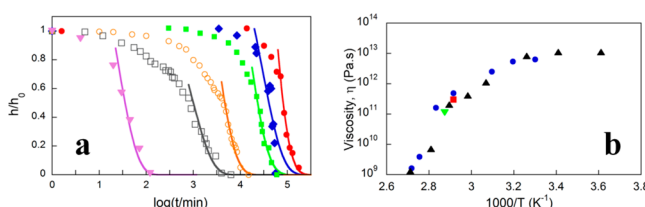


Figure 3. (a) Temporal evolution of the mean bump height for surfaces nanostructured at 25 °C stored at different temperatures. Triangles: 90 °C; open squares: 80 °C; open circles: 70 °C; closed squares: 50 °C; rhombus: 40 °C; closed circles: 30 °C. The continuous lines correspond to least-squares fits to exponential decay of the data at times longer than the decay time. (b) Polymer surface η vs T . This work (blue circles). Similar results were obtained in a study of relaxation of nanoholes (black triangles³²), from the decay of surface roughness (inverted triangle³⁷), or surface corrugation (squares³¹).

expected, the relaxation time markedly decreases with increasing temperature. However, while at $T > 70$ °C τ varies significantly with temperature, its T dependence becomes much weaker at lower T . The leveling of irregularities in viscous and viscoelastic films has been extensively discussed in the literature.^{29,30} The process is determined by the action of capillary (surface tension driven) and viscoelastic forces. At short times viscous and elastic forces must be considered. On the contrary, at times longer than the relaxation time of the film only viscous forces are relevant, and the stress decays nearly exponentially with a characteristic time given by $\tau_c \sim \eta\lambda/\gamma$, where η and γ are the viscosity and surface tension of the film and λ is the characteristic size of the deformation, as expected for a viscous liquid.³⁰ Thus, we can estimate the zero shear viscosity of the films from the measured decay times, as has been recently reported in studies of relaxation of gratings-shaped surfaces³¹ or nanoholes.³² As can be observed in Figure 3b, our results closely agree with previously reported data measured by following different experimental protocols. For temperatures higher than 65 °C ($\sim T_g - 30$ °C) η falls below 10^{12} Pa·s—the common operational convention for T_g in bulk—decreasing by 3 orders of magnitude at $T \sim T_g$. Thus, a significant reduction in T_g near the surface is observed. More interestingly, no divergence of η was observed at low temperatures. The subexponential η (or τ) growth with $1/T$ suggests a decreasing energy barrier with decreasing temperature. This behavior is the opposite of what is typically observed in 3D samples: bulk α - and β -relaxations show Arrhenius-like behavior below T_g ,^{32–34} even though α or β peaks extend several decades on frequency (or time), their characteristic time increases exponentially with $1/T$. Analogously, an exponential growth of the characteristic time was observed in dewetting studies of thick PS films.³⁵ The unusual sub-Arrhenius behavior observed here could be attributed to a reduction of the typical volume susceptible to rearrange in concert with decreasing T , resulting in a decreasing energy barrier for the thermally activated relaxation. However, under

the light of the results described above, it appears more reasonable to link the continuous decrease of $d \log(\tau)/d(1/T)$ to the gradually changing influence of zones of very different viscoelastic properties (even though the films were homogeneous at the moment of the structuration). At high T the relative weight of zones of low μ leads to Arrhenius-like behavior. At low T the predominance of zones of high μ leads to the observed athermal behavior. It could also be the case that slow evolution of residual stresses in the film affects the viscosity estimation, by making our assumption of purely viscous driven relaxation invalid at low temperatures. More elaborated studies—with carefully controlled aging protocols—will be necessary to clarify this point.

In a second test, we studied the evolution of polymer surfaces at $T = 30$ °C after structuration at different T . As was discussed above, changing the temperature of treatment modifies the resulting structured morphology. This change has some consequences on the temporal evolution of the structured films, as can be observed in Figure 4. As the bump distribution

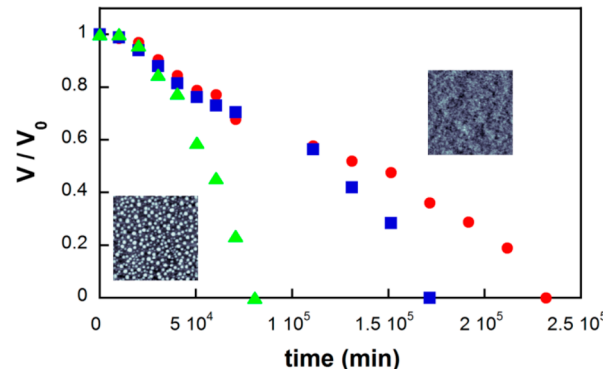


Figure 4. Temporal evolution of the total bump volume for surfaces nanostructured at 30 °C (triangles), 50 °C (squares), and 70 °C (circles) and aged at 30 °C. Inset: typical $1 \times 1 \mu\text{m}^2$ AFM height micrographs measured in air before and after relaxation of the structure.

is not always monomodal (cf. Figure 1), it is not convenient in this case to describe the film relaxation using the mean bump height. Instead, we determined the temporal evolution of the structured volume, defined as the total polymer volume above the flat level of the films. While a simple decay process is observed for the case of the monodisperse bumps, a significant deviation from this scenario is observed for the heterogeneous case: a description including at least two characteristic times appears to be necessary for the surfaces structured at 50 and 70 °C. In a study of the kinetic of enthalpy recovery, it has been recently reported that glassy polymers may have two different aging mechanisms with well-separated decay times.²⁷ However, it does not appear to be necessary to evoke different relaxation processes to describe the complex temporal evolution observed in this work: as can be inferred from Figure 4, the ratio between the different characteristic times is not larger than 3, which is consistent with the ratio between small and large bump sizes initially present in the structured films (cf. Figure 1). The short (long) time decay is related to the relaxation of the smaller (larger) bumps. Thus, films that were viscoelastically heterogeneous at the moment of structuration at high T exhibit a seemingly homogeneous η upon relaxation when aged at low T . These results, combined with the results of bump formation described above, reinforce the idea that the

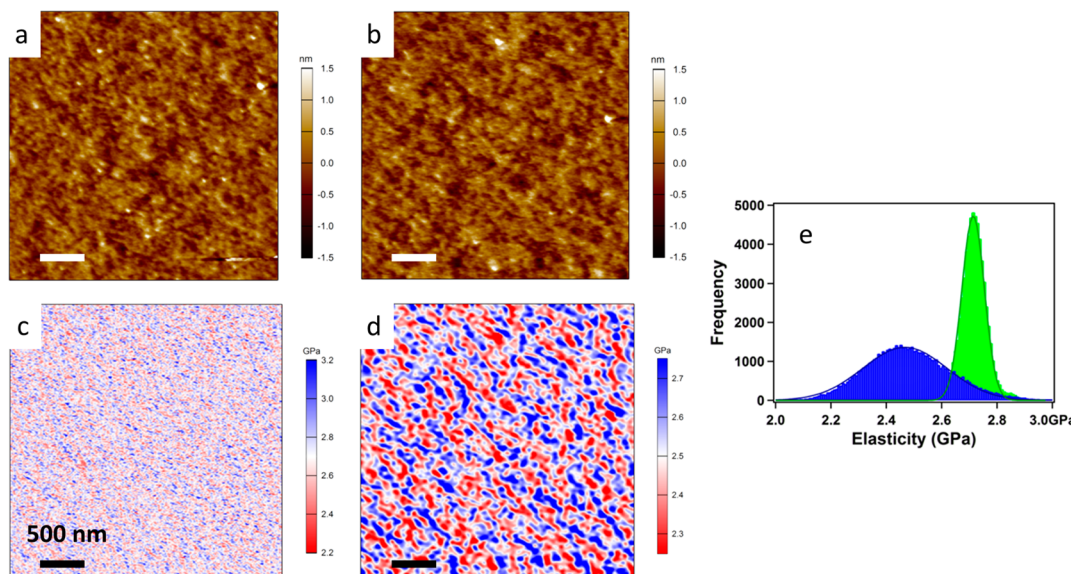


Figure 5. (a, b) Height and (c, d) elastic modulus maps of a PS film at (a, c) 30 °C and (b, d) 70 °C. (e) Number distribution of the apparent elastic modulus at 30 °C (green) and 70 °C (blue).

heterogeneity observed at larger T is not a consequence of quenching down a dynamically heterogeneous liquid, but a temperature-dependent property of the films. The film goes through a real change of viscoelastic properties, characterized by a change in the typical length scales of the observed modulus variation (see below), that cannot be explained in terms of a uniform “effective” temperature.

One puzzling aspect of the results reported in this article is the large difference in bump size observed at large T (Figures 1 and 2). As discussed above, we could attribute this to spatially variable elastic properties of the polymer surface. To further explore this point, we mapped the elastic modulus of a 247 nm thick PS film at two temperatures, by the method described in the Materials and Methods section. It is important to emphasize that for this experiment the film has not been subjected to any further treatment after the initial annealing at high T . The results are presented in Figure 5. As can be observed in the figure, the topography of the film (insets) is spatially homogeneous at both temperatures; the R.M.S. roughness is smaller than 1 nm, and no spatial structure can be identified. On the contrary, important temperature dependence can be observed in the modulus maps. While at low temperature (Figure 5a) the measured modulus is rather homogeneous everywhere on the film (within the spatial resolution of our measurements), segregated patches with differentiated elastic modulus appear at high temperature. Soft and hard zones much larger than the molecular size can be identified in the map. As described in the Materials and Methods section, to build these maps it was necessary to use a sample of known elastic modulus to calibrate the response of the system. It is also assumed that the tip–substrate contact can be well described by Hertz model. However, variations in tip–substrate adhesion might also be responsible for the observed heterogeneity.

We cannot discard the possibility that at low temperatures there exist heterogeneity in the elastic modulus, with a characteristic length scale smaller than our experimental resolution (of the order of 5 nm). Indeed, a recent publication suggests this may be the case.³⁶ However, the histograms shown in Figure 5e evidence how the distribution of measured

modulus (or apparent modulus) becomes much broader at higher temperature. The clear formation of domains (mosaic-like structure) evidence a nonrandom distribution of viscoelastic properties on the polymer surface. Other aspects of these results are noteworthy. The fact that the high temperature map (Figure 5b, d) was measured after the one at low temperature (Figure 5a, c) clearly shows that the heterogeneous modulus observed is not the result of quenching a heterogeneous polymer melt. The observed heterogeneity appears to properly characterize the glassy film equilibrated at $T < T_g$. A second important aspect is related to the dynamic of the polymer film. Two minutes were necessary to complete the maps presented. In that time lapse the patches could be clearly identified and no variations in the modulus were detected, suggesting a slow evolution of the measured structure. However, a faster characterization of the modulus was beyond our experimental capabilities. The heterogeneity and the patchy aspect of the map measured at 70 °C seem to support our conclusions from the relaxation studies. On the contrary, the range of observed apparent local modulus at high temperature (between 2 and 3 GPa) appears insufficient to explain the range in bump sizes generated by IPN. Several reasons can be hypothesized to explain this discrepancy: either the heterogeneity of the surface is magnified by the water-based IPN treatment, or the coalescence of the formed bumps is accelerated in zones of lower modulus, enhancing the difference in the pattern size obtained.

In summary, by studying the nanostructuration of the films and relaxation of the surface patterns, we have evidenced the heterogeneity of the viscoelastic properties of the surface of PS films in a range of temperatures far below T_g . In addition, a broad distribution of local elastic modulus of the polymer surface well below the glass transition temperature was directly observed by AFM. The observed heterogeneity appears to be an intrinsic property of the films and not a consequence of quenching the properties of the supercooled melt that could be described by a global effective film temperature.

AUTHOR INFORMATION

Corresponding Author

*E-mail drummond@crpp-bordeaux.cnrs.fr (C.D.).

Notes

The authors declare no competing financial interest.

ACKNOWLEDGMENTS

We kindly acknowledge Ludger Weisser and Dr. Florian Johann, Asylum Research, for helping in performing AM-FM measurements and Arjen Pit for helping with AFM micrographs processing.

REFERENCES

- (1) Angell, C. A. Perspective on the Glass Transition. *J. Phys. Chem. Solids* **1988**, *49*, 863–871.
- (2) Kob, W. In *Slow Relaxations and Nonequilibrium Dynamics in Condensed Matter*; Jean-Louis Barrat, J.-L., Feigelman, M., Kurchan, J., Dalibard, J., Eds.; EDP Sciences: Paris, 2003; pp 199–269.
- (3) Cavagna, A. Supercooled Liquids for Pedestrians. *Phys. Rep.* **2009**, *476*, 51–124.
- (4) Cangialosi, D. Dynamics and Thermodynamics of Polymer Glasses. *J. Phys.: Condens. Matter* **2014**, *26*, 153101.
- (5) Schiener, B.; Bohmer, R.; Loidl, A.; Chamberlin, R. V. Nonresonant Spectral Hole Burning in the Slow Dielectric Response of Supercooled Liquids. *Science* **1996**, *274*, 752–754.
- (6) Cicerone, M. T.; Ediger, M. Enhanced Translation of Probe Molecules in Supercooled o-Terphenyl: Signature of Spatially Heterogeneous Dynamics? *J. Chem. Phys.* **1996**, *104*, 7210.
- (7) Sillescu, H. Heterogeneity at the Glass Transition: A Review. *J. Non-Cryst. Solids* **1999**, *243*, 81–108.
- (8) Richert, R. Heterogeneous Dynamics in Liquids: Fluctuations in Space and Time. *J. Phys.: Condens. Matter* **2002**, *14*, R703–R738.
- (9) Ediger, M. D. Spatially Heterogeneous Dynamics in Supercooled Liquids. *Annu. Rev. Phys. Chem.* **2000**, 99–128.
- (10) Thirau, C. T.; Ediger, M. D. Spatially Heterogeneous Dynamics during Physical Aging Far below the Glass Transition Temperature. *J. Polym. Sci., Part B: Polym. Phys.* **2002**, *40*, 2463–2472.
- (11) Riggleman, R. A.; Lee, H.-N.; Ediger, M. D.; de Pablo, J. J. Heterogeneous Dynamics during Deformation of a Polymer Glass. *Soft Matter* **2010**, *6*, 287.
- (12) Vallée, R. A. L.; Cotlet, M.; Hofkens, J.; De Schryver, F. C.; Müllen, K. Spatially Heterogeneous Dynamics in Polymer Glasses at Room Temperature Probed by Single Molecule Lifetime Fluctuations. *Macromolecules* **2003**, *36*, 7752–7758.
- (13) Siretanu, I.; Chapel, J. P.; Drummond, C. Water-Ions Induced Nanostructuration of Hydrophobic Polymer Surfaces. *ACS Nano* **2011**, *5*, 2939–2947.
- (14) Siretanu, I.; Chapel, J.-P.; Bastos-González, D.; Drummond, C. Ions-Induced Nanostructuration: Effect of Specific Ionic Adsorption on Hydrophobic Polymer Surfaces. *J. Phys. Chem. B* **2013**, *117*, 6814–6822.
- (15) Siretanu, I.; Chapel, J. P.; Drummond, C. Substrate Remote Control of Polymer Film Surface Mobility. *Macromolecules* **2012**, *45*, 1001–1005.
- (16) Chapel, J.-P.; Rao, A.; Zong, Z. Modified Surfaces and Method for Modifying a Surface, 2007/126925 A2, 2007.
- (17) Labuda, A.; Kobayashi, K.; Miyahara, Y.; Grütter, P. Retrofitting an Atomic Force Microscope with Photothermal Excitation for a Clean Cantilever Response in Low Q Environments. *Rev. Sci. Instrum.* **2012**, *83*, 053703.
- (18) Gannepalli, A.; Yablon, D. G.; Tsou, A. H.; Proksch, R. Mapping Nanoscale Elasticity and Dissipation Using Dual Frequency Contact Resonance AFM. *Nanotechnology* **2011**, *22*, 355705.
- (19) Garcia, R.; Proksch, R. Nanomechanical Mapping of Soft Matter by Bimodal Force Microscopy. *Eur. Polym. J.* **2013**, *49*, 1897–1906.
- (20) Sarkar, J.; Sharma, A. A Unified Theory of Instabilities in Viscoelastic Thin Films: From Wetting to Confined Films, from Viscous to Elastic Films, and from Short to Long Waves. *Langmuir* **2010**, *26*, 8464–8473.
- (21) Huang, S.-Q.; Li, B.; Feng, X.-Q. Three-Dimensional Analysis of Spontaneous Surface Instability and Pattern Formation of Thin Soft Films. *J. Appl. Phys.* **2008**, *103*, 083501.
- (22) De Gennes, P. G. Glass Transitions in Thin Polymer Films. *Eur. Phys. J. E* **2000**, *2*, 201–205.
- (23) Priestley, R. D.; Ellison, C. J.; Broadbelt, L. J.; Torkelson, J. M. Structural Relaxation of Polymer Glasses at Surfaces, Interfaces, and in Between. *Science* **2005**, *309*, 456–459.
- (24) Keddie, J. L.; Jones, R. A. L.; Cory, R. A. Size-Dependent Depression of the Glass Transition Temperature in Polymer Films. *Europhys. Lett.* **1994**, *27*, 59–64.
- (25) Adam, G.; Gibbs, J. H. On the Temperature Dependence of Cooperative Relaxation Properties in Glass-Forming Liquids. *J. Chem. Phys.* **1965**, *43*, 139.
- (26) Schmidt-Rohr, K.; Spiess, H. Nature of Nonexponential Loss of Correlation above the Glass Transition Investigated by Multidimensional NMR. *Phys. Rev. Lett.* **1991**, *66*, 3020–3023.
- (27) Cangialosi, D.; Boucher, V. M.; Alegre, A.; Colmenero, J. Direct Evidence of Two Equilibration Mechanisms in Glassy Polymers. *Phys. Rev. Lett.* **2013**, *111*, 095701.
- (28) Ritort, F.; Sollich, P. Glassy Dynamics of Kinetically Constrained Models. *Adv. Phys.* **2003**, *52*, 219–342.
- (29) Orchard, S. On Surface Levelling in Viscous Liquids and Gels. *Appl. Sci. Res., Sect. A* **1963**, *11*, 451–464.
- (30) Keunings, R.; Bousfield, D. W. Analysis of Surface Tension Driven Leveling in Viscoelastic Films. *J. Non-Newtonian Fluid Mech.* **1987**, *22*, 219–233.
- (31) Buck, E.; Petersen, K.; Hund, M.; Krausch, G.; Johannsmann, D. Decay Kinetics of Nanoscale Corrugation Gratings on Polymer Surface: Evidence for Polymer Flow below the Glass Temperature. *Macromolecules* **2004**, *37*, 8647–8652.
- (32) Fakhraai, Z.; Forrest, J. A. Measuring the Surface Dynamics of Glassy Polymers. *Science* **2008**, *319*, 600–604.
- (33) McCrum, N. G.; Read, B. E.; Williams, G. *Anelastic and Dielectric Effects in Polymeric Solids*; Wiley: London, 1967.
- (34) Dhinojwala, A.; Wong, G. K.; Torkelson, J. M. Rotational Reorientation Dynamics of Disperse Red 1 in Polystyrene: A Relaxation Dynamics Probed by Second Harmonic Generation and Dielectric Relaxation. *J. Chem. Phys.* **1994**, *100*, 6046.
- (35) Chowdhury, M.; Freyberg, P.; Ziebert, F.; Yang, A. C.-M.; Steiner, U.; Reiter, G. Segmental Relaxations Have Macroscopic Consequences in Glassy Polymer Films. *Phys. Rev. Lett.* **2012**, *109*, 136102.
- (36) Nguyen, H. K.; Wang, D.; Russell, T. P.; Nakajima, K. Observation of Dynamical Heterogeneities and Their Time Evolution on the Surface of an Amorphous Polymer. *Soft Matter* **2015**, *11*, 1425–1433.
- (37) Kerle, T.; Lin, Z.; Kim, H.; Russell, T. P. Mobility of Polymers at the Air/Polymer Interface. *Macromolecules* **2001**, *34*, 3484–3492.